



POLİTEKNİK DERGİSİ

JOURNAL of POLYTECHNIC

ISSN: 1302-0900 (PRINT), ISSN: 2147-9429 (ONLINE)

URL: <http://dergipark.org.tr/politeknik>



A deep learning based automatic cerebral aneurysm detection in brain computed tomography angiography scan images

Beyin bilgisayarlı tomografi anjiyografi tarama görüntülerinde derin öğrenme tabanlı otomatik serebral anevrizma tespiti

Yazar(lar) (Author(s)): Meltem YAVUZ ÇELİKDEMİR¹, Ayhan AKBAL²

ORCID¹: 0000-0003-0552-2601

ORCID²: 0000-0001-5385-9781

To cite to this article: Yavuz Çelikdemir M., Akbal A., “A Deep Learning Based Automatic Cerebral Aneurysm Detection in Brain Computed Tomography Angiography Scan Images”, *Journal of Polytechnic*, *(*) : *, (*).

Bu makaleye şu şekilde atıfta bulunabilirsiniz: Yavuz Çelikdemir M., Akbal A., “A Deep Learning Based Automatic Cerebral Aneurysm Detection in Brain Computed Tomography Angiography Scan Images”, *Politeknik Dergisi*, *(*) : *, (*).

Erişim linki (To link to this article): <http://dergipark.org.tr/politeknik/archive>

DOI: 10.2339/politeknik.1261854

A Deep Learning Based Automatic Cerebral Aneurysm Detection in Brain Computed Tomography Angiography Scan Images

Highlights

- ❖ It is implemented by changing the parameters of the deep neural network.
- ❖ In general, it reduces the number of iterations, it requires low GPU or CPU.
- ❖ Detects of brain aneurysms on computed tomography angiography.
- ❖ It guides neurosurgeons and radiologists.
- ❖ All comparable results are given numerically.

Graphical Abstract

Bu çalışmada BTA görüntüler kullanılarak derin öğrenme modeli ile serebral anevrizma sınıflandırması yapılmıştır. In this study, cerebral aneurysm classification was performed with deep learning model using CTA images

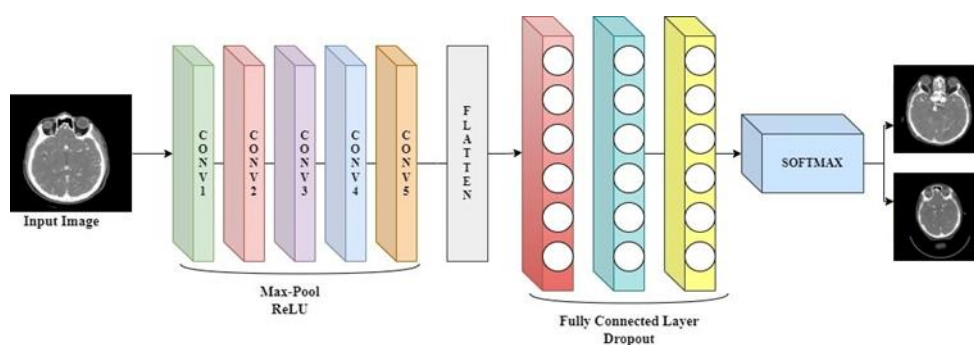


Figure. Classification of cerebral aneurysm

Aim

Minimizing the interpretation errors in CTA images of radiologists

Design & Methodology

Aneurysm classification was made in CTA image analysis by applying deep learning model with Convolutional Neural Network.

Originality

Using a new data set that is not available in the literature, the training has a high rate of validation with 99.54% accuracy, 98% sensitivity, 100% specificity, and 100% precision, and testing is done with 100% accuracy.

Findings

For images of patients with aneurysm, 127 true positives, 1 false positive, and 89 true negatives and 0 false negative for images of patients with non-aneurysm were evaluated.

Conclusion

Classification results were 99.2% for images with aneurysms and 100% for images with non-aneurysms.

Declaration of Ethical Standards

The authors of this article declare that the materials and methods used in this study do not require ethical committee permission and/or legal-special permission.

A Deep Learning Based on Automatic Cerebral Aneurysm Detection in Brain Computed Tomography Angiography Scan Images

Araştırma Makalesi / Research Article

Meltem YAVUZ ÇELİKDEMİR^{1*}, Ayhan AKBAL²

¹ Bitlis Eren University, Tatvan Vocational High School, Electric and Energy, Türkiye

² Firat University, Engineering Faculty, Electrical and Electronics Engineering, Türkiye

(Geliş/Received : 08.03.2023 ; Kabul/Accepted : 22.03.2024 ; Erken Görünüm/Early View : 10.06.2024)

ABSTRACT

Cerebral aneurysms are an important disease that threatens human life. Rupture of these aneurysms causes hemorrhages in the cerebral arteries. Computed Tomography Angiography (CTA) is widely used in the clinical diagnosis of cerebral aneurysms. Interpretation errors by radiologists in examining these Computed Tomography (CT) images are vital for patients. Based on this importance, deep learning-based studies aim to help keep these errors to a minimum. For this purpose, CTA images were used to detect cerebral aneurysms in this study. For CTA image analysis, deep learning methodology was preferred through Convolutional Neural Network (CNN). The validation accuracy of the training obtained as a result of deep learning has a high rate of validation with 99.54% accuracy, 100% sensitivity, 98.89% specificity and 100% precision. As a training dataset, it yielded 127 true positives and 1 false positive for patient images with aneurysm, 89 true negatives and 0 false negative for images of patients with non-aneurysms. In this trained network, results were obtained with a high accuracy of 86.6% on 75 CTA images for external test. Regional dimension analysis was also performed for an image with an aneurysm detected in the test process.

Keywords: Deep learning, cerebral aneurysm, CTA-scan image.

Beyin Bilgisayarlı Tomografi Anjiyografi Tarama Görüntülerinde Derin Öğrenme Tabanlı Otomatik Serebral Anevrizma Tespiti

ÖZ

Serebral anevrizmalar, insan hayatını tehdit eden önemli bir hastalıktır. Bu anevrizmaların rüptüre olması beyin arterlerinde kanamalara sebep olmaktadır. Klinik olarak serebral anevrizmaların tanısında bilgisayarlı tomografi anjiyografi yaygın olarak kullanılmaktadır. Bununla birlikte radyoloji uzmanlarının tomografi görüntülerini yorumlama hataları hastalar için hayati öneme sahiptir. Bu öneme binaen yapılan derin öğrenme tabanlı çalışmalar bu hataları minimum seviyede tutmaya yardımcı olmayı amaçlamaktadır. Bu amaç doğrultusunda yapılan bu çalışmada serebral anevrizmaların tespiti için BTA görüntüleri kullanılmıştır. BTA görüntü analizleri için ise Evrişimli Sinir Ağı aracılığı ile derin öğrenme metodolojisi tercih edilmiştir. Derin öğrenme sonucunda elde edilen eğitimin doğrulama doğruluğu %99.54, duyarlılığı %98, özgüllüğü %100, hassaslığı %100 ile yüksek orana sahiptir. Eğitim veri seti olarak, anevrizmalı hasta görüntüleri için 127 doğru pozitif, 1 yanlış negatif, anevrizmasız hasta görüntüleri için 89 doğru pozitif, 0 yanlış pozitif olarak sonuç vermiştir. Eğitilmiş ağda, harici test için 75 CTA görüntüde %86.6 gibi yüksek bir doğrulukla sonuçlar elde edildi. Test işleminde anevrizma tespit edilen bir görüntü için bölgesel boyut analizi yapılmıştır.

Anahtar Kelimeler: Derin öğrenme, serebral anevrizma, BTA-tarama görüntüsü.

1. INTRODUCTION

Cerebral aneurysms are a focal expansion in the cerebral artery that develops in the form of a bubble outward at the site of the weakening of the vessel wall [1]. Cerebral aneurysms can be found in different locations. These locations are; Middle Cerebral Artery (MCA), Internal Carotid Artery (ICA), Posterior Inferior Cerebral Artery (PICA), Anterior Cerebral Artery (ACA), Anterior

Communicating Artery (ACOMA). These aneurysms are a serious risk factor for patients' health and constitute 3-7% of the population [2-5]. In this context, early diagnosis and treatment of cerebral aneurysms is an important issue [6]. Accurate diagnosis of brain aneurysms is a topic frequently addressed by researchers [3,4]. In the studies reviewed by the researchers, a deep learning model was used to detect automatic aneurysm in DSA images. Using 75, 20, and 35 image data for the training set, internal test set, and external test set, respectively, the sensitivity was 94.4% for the internal

*Sorumlu yazar (Corresponding Author)
e-posta : meltem.ycd@gmail.com

test and 82.9% for the external test [7]. Computed Tomography (CT), which is one of the neurological imaging methods for cerebral aneurysms, is widely used in the diagnosis of aneurysms. Computed Tomography Angiography (CTA) includes advanced CT software-based images that show cerebral vessels in three dimensions. The new image obtained in a short time can be checked for surgical planning. This new image contains images of the brain, skull bones or vascular structure. CTA and Magnetic Resonance Angiography (MRA) are recommended as the first approach in the detection of non-ruptured aneurysms due to their less invasive nature [8].

In the studies, deep learning, machine learning and artificial intelligence-based methods are becoming widespread for the diagnosis and detection of diseases in the field of health. Semi-automatic artificial intelligence-based programs are used to detect non-ruptured brain aneurysms [9]. In later studies, it was aimed to distinguish ruptured aneurysms from non-ruptured aneurysms with the machine learning model [10]. Potentials and limitations have been applied in deep learning-based studies conducted from past to present for brain computed tomography [11]. Convolutional Neural Network (CNN) based architecture was applied to detect intracranial aneurysms in Digital Subtraction Angiography (DSA) images, achieving 93.5% accuracy [12]. Posterior communicating artery aneurysms were detected in 2D DSA images with 91% accuracy by deep learning diagnosis system [13]. Similarly, 92.82% sensitivity was achieved by using U-Net structure to detect intracranial aneurysms in DSA images [14]. Transcranial Doppler images were analyzed and VGG16 was administered to detect aneurysm in the Middle Cerebral Artery (MCA) to achieve 84% sensitivity [15]. Region-Based Convolutional Neural Network (RCNN) model was used for automatic detection of aneurysms and the sensitivity was calculated as 96.7% [16]. 3D-UNet was applied for the detection of brain aneurysm using Time-of-Flight Magnetic Resonance Angiography (TOF-MRA) images and 83% sensitivity was obtained [17].

Manual scanning of the aneurysm in CTA images requires different systems that give faster and more accurate results with regard to time and interpretation error [6]. Due to the need, the rapid development in technology has contributed to the increase in the number of artificial intelligence and deep learning-based approaches to automatically detect cerebral aneurysms [9,11].

Motivation of Study:

In the studies conducted in the literature, ready-made datasets were mostly used [17–20]. Deep learning studies using these ready datasets give a high accuracy rate. However, accuracy rates decrease when real datasets are preferred. A deep learning algorithm has been proposed

by researchers using TOF-MRA ready dataset for aneurysm detection [17]. In addition, aneurysm detection was performed by evaluating DSA images in the ready dataset obtained from the Cerebral Aneurysm Detection and Analysis (CADA) competition [18]. Other studies have similar content [20–23].

The motivation of the study, a new dataset that is not available in the literature was used. For this, images of dataset were randomly determined into 217 images in the internal test set, 508 images in the training set and 75 images were used for the external test set. A higher accuracy rate was obtained by using an external test set that used more data sets from the literature. In addition, the most important feature of the dataset is that it consists of CTAs and has high sensitivity in determining the vessel structure. Failure to use ready data is a disadvantage for the CNN preferred in the study. In the proposed model, pre-trained AlexNet is used for deep feature extraction.

In this study, our main goal is to perform a deep learning study using brain CTA images for automatic detection of brain aneurysms. The study conducted with the deep learning method developed in this way was carried out in four stages. Firstly, a dataset consisting of images of healthy patients with non-aneurysms and diseased patients with aneurysms in different locations and sizes was created. This dataset was obtained from CTA images of patients. In the second stage, a deep learning model was developed to detect the aneurysm on the images. For this purpose, classification process was performed on CTA images. In the third stage, the performance analysis of the system was made and the accuracy, specificity, sensitivity and precision parameter values were examined. In the last stage, regional dimension analysis was performed for an image with aneurysm diagnosed on test images.

2. MATERIAL and METHOD

Brain CTA images are acquired in different image planes. These image planes are classified as axial, sagittal and coronal sections. In this study, brain CTA coronal images were used as the input image preference on CNN. Coronal images have been preferred as they contain more sensitive images. AlexNet was preferred among deep learning-based CNN architectures to detect patients with cerebral aneurysm. The reason for this preference is that AlexNet architecture gives more accurate results [20]. Coronal images obtained for use in AlexNet architecture were resized by preprocessing. The first layers of the AlexNet architecture evaluate and create labels for each of the categories such as color and line in brain CTA images. Transfer learning is used in the pre-trained network because it is difficult in terms of time and operation to train the network with random weights to learn a new task. The architecture of the methodology used for image classification of aneurysms and non-aneurysms is shown in Figure 1.

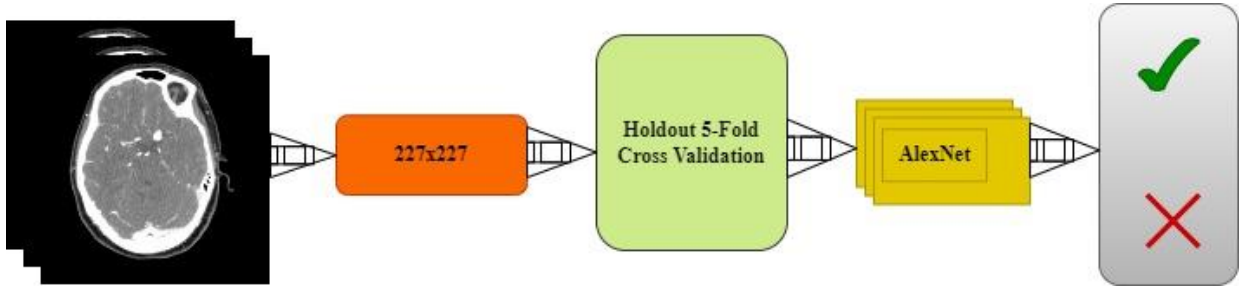


Figure 1. Architecture of the proposed method

AlexNet is defined as a pre-trained CNN. The layers and weight values of the network are given in Table 1. AlexNet architecture is 8 layers deep, evaluating images in 1000 different categories. This architecture includes 5 convolutional layers and 3 fully connected layers. The first layer is the input layer and the image data is “227 x 227 x 3”. Here, “227 x 227” represents the resolution and 3 represents the number of color channels. In the presented study, the last three layers of AlexNet were changed and fine-tuned. The deep learning model

transferred as a result of this change is called transfer learning. Transfer learning is a suitable method when there are not enough examples when training a deep neural network. Using all the parameters available in the pre-trained network increases the training time. This only requires using a high-performance GPU or CPU. Transfer learning was done to shorten the training time and apply it on our personal computer, and this problem was solved.

Table 1. Layers and weights of AlexNet

Code	Layer Name	Activations	Weights
'data'	Image Input	227x227x3	-
'conv1'	Convolution	55x55x96	11x11x3x96 Stride [4 4] Padding [0 0 0 0]
'relu1'	ReLU Activation	55x55x96	-
'norm1'	Cross Channel Normalization	55x55x96	-
'pool1'	Max Pooling	27x27x96	Stride [2 2] Padding [0 0 0 0]
'conv2'	Grouped Convolution	27x27x256	5x5x48x128 Stride [1 1] Padding [2 2 2 2]
'relu2'	ReLU Activation	27x27x256	-
'norm2'	Cross Channel Normalization	27x27x256	-
'pool2'	Max Pooling	13x13x256	Stride [2 2] Padding [0 0 0 0]
'conv3'	Convolution	13x13x384	3x3x256x384 Stride [1 1] Padding [1 1 1 1]
'relu3'	ReLU Activation	13x13x384	-

Table 2(contunie). Layers and weights of AlexNet

'conv4'	Grouped Convolution	13x13x384	3x3x192x192 Stride [1 1] Padding [1 1 1 1]
'relu4'	ReLU Activation	13x13x384	-
'conv5'	Grouped Convolution	13x13x256	3x3x192x128 Stride [1 1] Padding [1 1 1 1]
'relu5'	ReLU Activation	13x13x256	-
'pool5'	Max Pooling	6x6x256	Stride [2 2] Padding [0 0 0 0]
'fc6'	Fully Connected	1x1x4096	4096x9216
'relu6'	ReLU Activation	6x6x256	-
'drop6'	Dropout	6x6x256	50%
'fc7'	Fully Connected	1x1x4096	4096 Fully Connected Layer
'relu7'	ReLU Activation	6x6x256	-
'drop7'	Dropout	6x6x256	50% Dropout
'fc8'	Fully Connected	1x1x4096	1000 Fully Connected Layer
'prob'	Softmax	1x1x1000	Softmax
'output'	Classification Output	2	Crossentropyex with 'Tench' and 999 Other Classes

If it is necessary to define some of the layers according to the order of operation in the network architecture;

Convolution layer is the first layer that evaluates the image. Filtering is applied by moving the convolution matrix consisting of certain pixels on the image. It is used for feature extraction and reduction in the image. In this layer, the features of the image are learned. The working principle for the convolution layer is given in Figure 2.

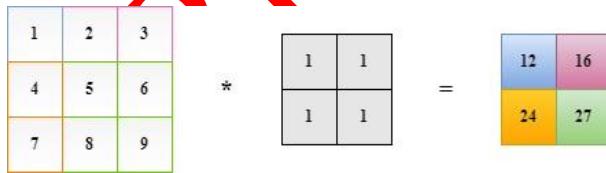


Figure 2. Working principle of the convolution layer

ReLU activation layer is a nonlinear function, which can be expressed as

$$f(x) = \begin{cases} x, & x > 0 \\ 0, & x \leq 0 \end{cases} \quad (1)$$

The purpose of using this layer is to prevent the model from learning negative values. In this layer, all negative values are set to 0.

Pooling layer increases learning speed by reducing dimensionality. There are two types as maximum and minimum pooling. These are the maximum pooling and average pooling methods. Maximum pooling takes the largest value in the filter footprint and average pooling reduces size by averaging the values. In the study, maximum pooling was used to decompose important features, as there was closeness between pixel values. In the pooling layer, the number of stride was taken as 2 pixels and the application was carried out [24]. The working principle for the pooling layer with matrix dimensions of 2x2 is given in Figure 3.

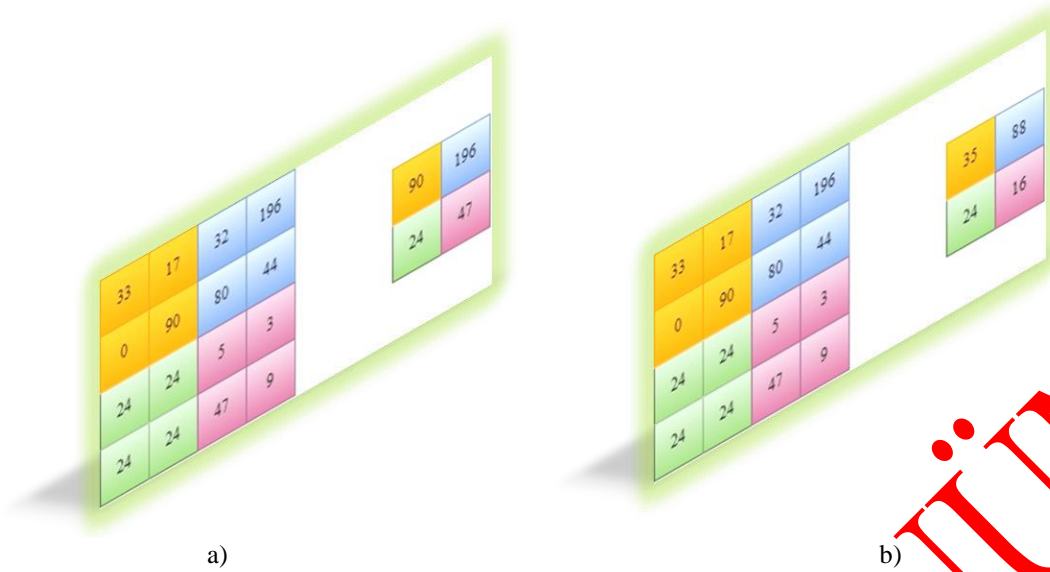


Figure 3. Working principles of pooling layer a)Max-pool b)Average-pool

Convolution and pooling layer can be added consecutively. After the pooling layer, the image, which is turned into a matrix, is converted into a vector by flattening. Figure 4 presented the matrix flattening.

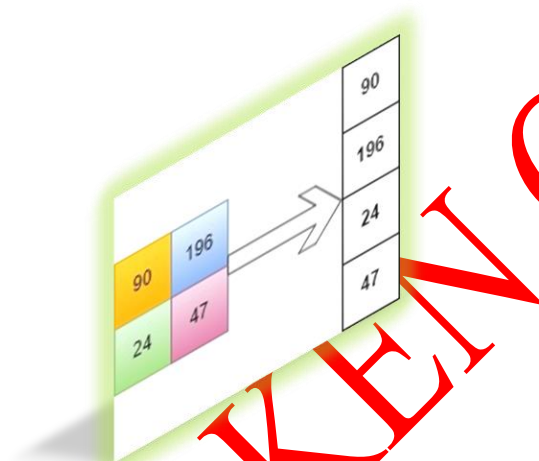


Figure 4. Matrix flattening

Fully connected layer; the flattened input image can be trained with neural networks and starts the learning process and is used for classification. It involves each neuron in the upper layer being connected to the next

layer neuron [25]. The working principle of this layer is given in Figure 5.

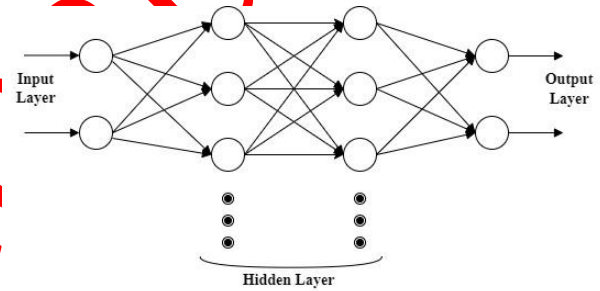


Figure 5. Working principle of fully connected layer

Softmax layer are vectors whose inputs can be positive, negative, or zero. It is the layer that converts a parameterless vector to a probability mass function. Activation function in this layer is defines as

$$x_i = \exp^{x_i} / \sum_{j=1}^d \exp^{x_j} \quad (2)$$

Softmax layer output is limited to (0,1) range and used as input to cross entropy loss. In the proposed model, the dataset has been cross-validated 5 times. The last layer is the decision stage of the classification process. Output information as aneurysm or non-aneurysm is obtained by evaluating the input image features. The architecture of the layers for the network used is given in Figure 6.

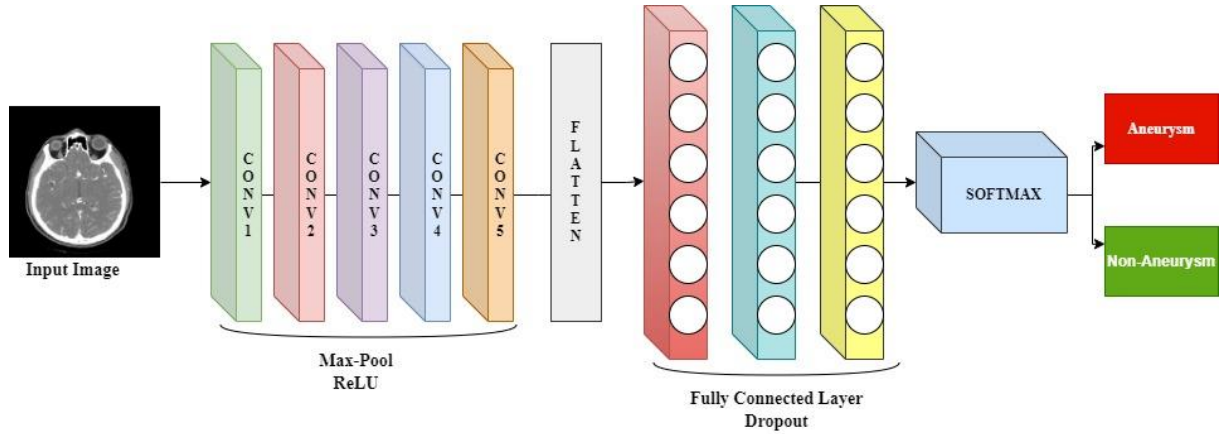


Figure 6. Layers of the network

3. EXPERIMENTAL FINDINGS

The image data was preprocessed and ready to be applied to the input of the network, and prediction was made on the trained network. Transfer learning is preferred to perform a deep learning model when there are not enough input images. Network training requires a high-performance GPU or CPU, while transfer learning takes place with ordinary CPU. CTA image data is processed in MATLAB program with 12-GB RAM and Intel Core i5 processor CPU. Image data was randomly selected as 70% for use in training and 30% for use in validation. Learning rate 1e-3, validation frequency 30, maximum epoch 8, minimum batch size 128 was chosen by using Momentum Stochastic Gradient Descent (SGDM) optimization in training. Training time is 4 minutes 46 seconds. At the end of the training, the input images are taken as two-class output images, aneurysm and non-aneurysm.

It is important to determine the area, diameter, major and minor axis length information for the aneurysm in CTA images. Due to this importance, dimensional analysis was performed in the aneurysm region.

3.1. Dataset

In this study, a dataset consisting of cerebral CTA images with coronal section was used. The dataset includes CTA images of patients treated in the neurosurgery outpatient clinic of Firat University Research Hospital in Türkiye between January 2011 and May 2021. The images that make up the dataset consist of aneurysm and non-aneurysm CTA images, agreed with the neurosurgeon and radiologist. Ethics committee approval was obtained from the hospital and the identity information written on the image was hidden for this study. Images in the dataset have “.dcm” file extensions and different sizes. All images were resized to “512 x 512”. Average voxel spacing for imaging data is 0.625 mm. The size of the presented aneurysms is in the range of 2-25 mm according to the radiology report results, which is a disadvantage for aneurysm detection. In this dataset, 51 aneurysm patients and 30 non-aneurysm patients consist

of a total of 81 patient images. There are 52 aneurysms in aneurysm images. Data augmentation was made on the images included in the training and a total of 725 images were obtained. The partitioning of the data set used in the study was made on an image basis. Training was carried out using 508 randomly selected images with a rate of 0.7%. Random CTA scan images were selected for testing. There are given images of aneurysm detected in CTA in Figure 7-a and non-aneurysm images Figure in 7-b.

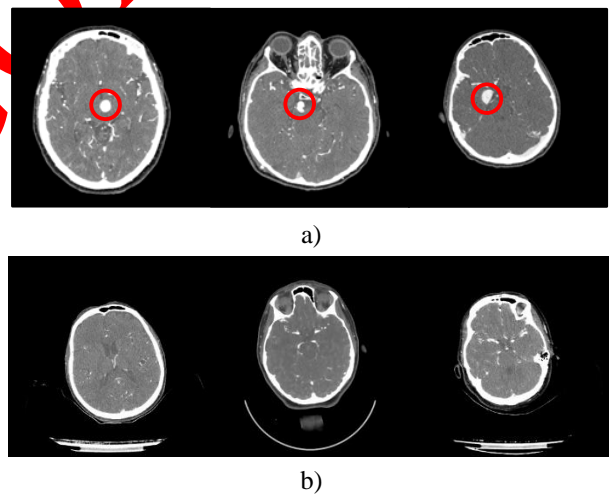


Figure 7. CTA images (a) Aneurysm (b) Non-aneurysm

CTA images were randomly selected as 508 and 217 images in the training and internal test set, respectively, and included in the study. In addition, 75 CTA images were used for external test. Automatic detection of aneurysms was performed on this external test dataset and the resulting accuracy was 86.6%.

3.2. Performance Analysis

Accuracy (Acc), sensitivity (SEN), specificity (SPE), and precision (PRC) parameters are used as criteria to evaluate

the performance of the system. Equation models for these parameters are defined as

$$A_{CC} = tp + tn/tp + tn + fp + fn \quad (3)$$

$$S_{EN} = tp/tp + fn \quad (4)$$

$$S_{PE} = tn/tn + fp \quad (5)$$

$$P_{RC} = tp/tp + fp \quad (6)$$

where, true positive (tp), true negative (tn), false positive (fp), false negative (fn) are the coefficients of the confusion matrix given in the next section. Sensitivity of

94.4% and false positive rate of 0.86 ($fp/case$) were obtained for 130 cases in automatic detection of intracranial aneurysms [7].

3.3. Regional Analysis

In this section, filtering techniques are applied on the CTA image of brain with aneurysm. For each determined region, parameters such as area, diameter, major and minor axis length were evaluated. Analysis results for different regions in the image are given in Table 2.

Table 3. Regional analysis values in aneurysm image

Area	Major length	axis	Minor length	axis	Eccentricity	Orientation	Euler number	Equiv diameter	Perimeter
9	4.0537		3.0245		0.6658	69.6994	1	3.3851	7.6830
43	19.6929		3.1790		0.9869	72.2377	1	7.3993	36.9840
20107	544.5650		436.2645		0.5985	-89.8562	26	160.0032	1.1833e+03
6	4.5135		2.0180		0.8945	77.0668	1	2.7640	6.9220
7	4.3128		2.2280		0.8562	81.6504	1	2.9854	6.9220
12	7.4240		2.4029		0.9462	75.4476	1	3.9088	12.7360
2	2.3094		1.1547		0.8660	0	1	1.5958	1.9600
29	7.7879		4.9812		0.7687	28.1718	1	6.0765	17.7150
9	4.4645		2.9007		0.7602	-60.4819	1	3.3851	8.3280
5	3.3066		2.1292		0.7651	71.5651	1	2.5231	4.9620
5	4.1633		1.8037		0.9013	45	1	2.5231	5.8140
3	3.4641		1.1547		0.9428	0	1	1.9544	3.9200
7	3.2367		3.0282		0.3531	0	1	2.9854	6.3680
8	3.6515		2.9721		0.5809	45	1	3.1915	6.8310
9	4.8483		2.7577		0.8225	76.7175	1	3.3851	8.7910
17	5.3090		4.2029		0.6110	15.1716	1	4.6524	11.4210
11	3.9848		3.8498		0.2581	45.0000	1	3.7424	9.2710
3	2.5820		1.7638		0.7303	-45	1	1.9544	3.0930
5	3.3066		2.1292		0.7651	71.5651	1	2.5231	4.9620
7	5.2621		1.9267		0.9306	-75.3211	1	2.9854	8.3280
49	13.1675		5.4442		0.9105	-2.2867	1	7.8987	28.9210
2	2.3094		1.1547		0.8660	90	1	1.5958	1.9600
1	1.1547		1.1547		0	0	1	1.1284	0
2	2.3094		1.1547		0.8660	90	1	1.5958	1.9600
38	11.0127		4.9151		0.8949	78.2896	1	6.9558	22.5610
690	32.2242		27.4340		0.5246	78.3438	1	29.6401	92.2540
53	13.3289		5.3000		0.9175	82.3240	1	8.2147	27.7710
4	2.3094		2.3094		0	0	1	2.2568	3.5560
46	10.8099		5.7052		0.8494	84.5456	1	7.6530	23.9670
11	4.1633		3.6560		0.4784	-18.4349	1	3.7424	8.9070

Table 4(contunie). Regional analysis values in aneurysm image

105	21.3362	6.3852	0.9542	2.4953	1	11.5624	42.7150
139	48.5130	10.5007	0.9763	-84.9655	1	13.3034	103.5260
2	2.3094	1.1547	0.8660	0	1	1.5958	1.9600
1	1.1547	1.1547	0	0	1	1.1284	0
2	2.3094	1.1547	0.8660	90	1	1.5958	1.9600
17	5.0906	4.4896	0.4714	-11.3099	1	4.6524	12.1570
13	4.4704	3.8564	0.5058	45	1	4.0684	9.4610
40	12.0072	4.4366	0.9292	-21.8474	1	7.1365	24.2480
5	3.5298	2.3594	0.7438	-55.9007	1	2.5231	5.8140
113	18.1906	10.1581	0.8296	-86.4420	1	11.9948	60.3720
25	8.5545	3.9892	0.8846	-42.7437	1	5.6419	17.5250
5	3.3066	2.1292	0.7651	18.4349	1	2.5231	4.9620
54	20.9619	3.7493	0.9839	69.6880	1	8.2919	39.2420
2	2.3094	1.1547	0.8660	90	1	1.5958	1.9600
9	4.0537	3.0245	0.6658	-20.3006	1	3.3851	7.6830
66	24.1704	3.7552	0.9879	-67.7214	1	9.1670	43.7490
6	4.5135	2.0180	0.8945	-77.0668	1	2.7640	6.9220

Accordingly, values for the region of aneurysm are shown in bold. In the study, the perimeter was calculated as 92.2540 units and the area as 690.0000 units for the values of the aneurysm. Image processing techniques have been applied to obtain a more distinct image of the aneurysm. Firstly, the image was preprocessed. The noise-free image is improved by applying compression

and filtering methods. Secondly, regional analysis of the aneurysm image was performed. Finally, a binary representation was performed for the aneurysm region. Staggered representation of the aneurysm area is given in Figure 8.

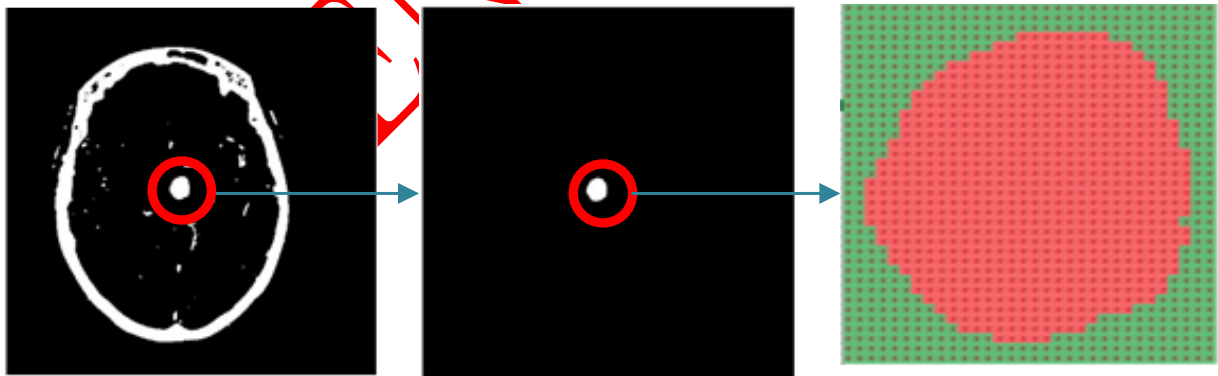


Figure 8. Binary representation for the aneurysm region

4. RESULTS

AlexNet completed the training in 286 seconds with 48 iterations to classify aneurysm and non-aneurysm images. The highest classification accuracy for AlexNet was achieved at 99.54%. The training graphs that find the

highest classification accuracy for AlexNet are given in Figure 9. Where, the blue curve represents the training accuracy and the red curve represents the training loss.

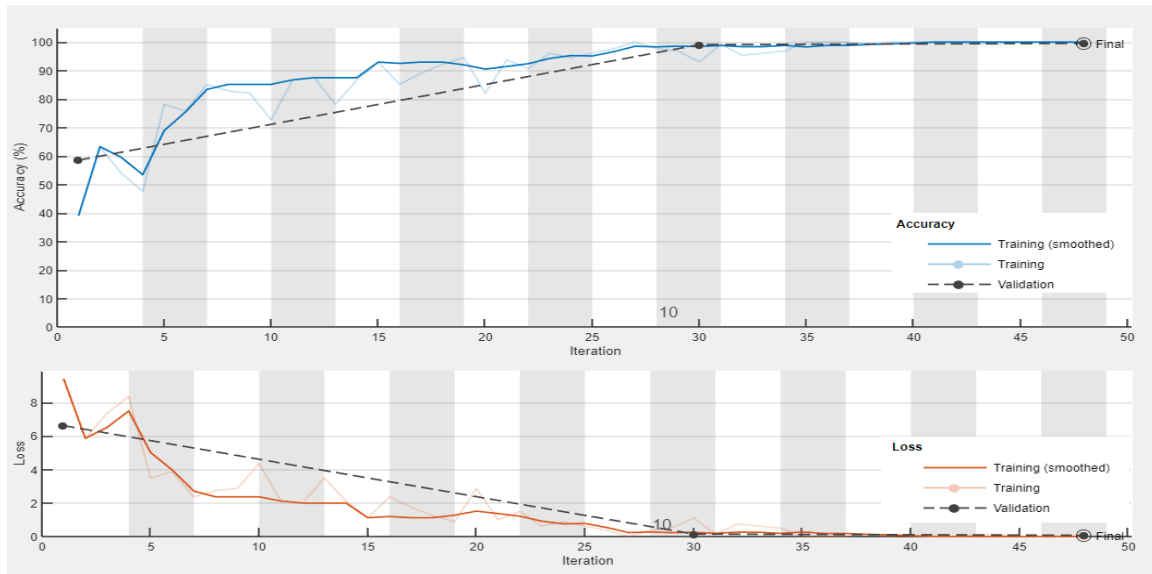


Figure 9. Training graphics

Training was carried out with different approaches and number of iterations on each epoch. The confusion matrix obtained for AlexNet is given in Figure 10. Using values from the confusion matrix, accuracy, sensitivity, specificity and precision are calculated. False negatives are shown in red and true positives in green. Performance analysis was performed with 127 true positives (tp) and 1 false positive (fp) in aneurysm images, and 89 true negatives (fn) and 0 false negatives (tn) in non-aneurysm images. As a result of the analysis, the highest 99.54% accuracy, 100% sensitivity, 98.89% specificity, and 100% precision were calculated.

		Confusion Matrix		
		aneurysm	non-aneurysm	
Output Class	aneurysm	127 58.9%	1 0.5%	99.2% 0.8%
	non-aneurysm	0 0.0%	89 41.0%	100% 0.0%
		aneurysm	non-aneurysm	99.5% 0.5%
		Target Class		

Figure 10. Confusion matrix

Aneurysm disease creates the risk of cerebral hemorrhage, so it must be detected very quickly and accurately. In this article, deep learning study was conducted with pre-trained AlexNet to classify CTA images for screening of cerebral aneurysms. In the

presented method, classification was made with the highest known accuracy rate of 99.54%. The limitation of the presented study is that it only consists of a dataset consisting of images of patients with aneurysms. It is necessary to examine different CTA images to detect other diseases and to compare the classification accuracy in deep learning.

5. CONCLUSION

CTA images consist of images of patients with cerebral aneurysm and non-aneurysm. Deep learning applications are widely used with developing technology to diagnose aneurysm in CTA images. In this study, aneurysm scanning was performed using AlexNet with our dataset consisting of brain CTA images. The layers of the pre-trained network were changed and the training accuracy of the network succeeded to achieve the highest known accuracy with 99.54%. In the internal test procedure, the classification results were 100% in non-aneurysm images and 99.2% in aneurysm images. In the external test process, better results were obtained than the literature with a high accuracy of 86.6%. It is predicted that if this network structure becomes an element of choice for screening different diseases, it will provide support in rapid diagnosis. In future studies, it is aimed to determine the risk of rupture based on hemodynamic factors for these aneurysms in different locations..

6. DISCUSSION

Deep learning models provide successful results on large data sets. Although a small number of data was used in this study, the number of images was increased with the image selections obtained from the video format of CTA images, thus increasing the accuracy in learning. In addition, it is normal for the results obtained in the study to be used in practical applications. Increasing studies on

detecting aneurysms and increasing accuracy with image processing methods will make a significant contribution to the literature. Additionally, this will provide significant guidance to neurosurgeons and radiologists. In addition to this, parameters related to rupture conditions in aneurysms will be added in the future and can be used to decide on surgical intervention. The fact that neurosurgeons and radiologists guide the detection and treatment of aneurysm disease emphasizes the importance of the study.

ACKNOWLEDGEMENT

The authors would like to thank Sait Öztürk for his contribution to CTA scan images.

DECLARATION OF ETHICAL STANDARDS

The authors of this article declare that the materials and methods used in this study do not require ethical committee permission and/or legal-special permission.

AUTHORS' CONTRIBUTIONS

Meltem YAVUZ ÇELİKDEMİR: Conceptualization, Investigation, Writing – review & editing, Software, Methodology, Validation, Formal analysis, Writing – original draft, Visualization, Data curation, Supervision, Project administration, Resources.

Ayhan AKBAL: Conceptualization, Investigation, Writing – review & editing, Software, Methodology, Validation, Formal analysis, Writing – original draft, Visualization, Data curation, Supervision, Project administration, Resources.

CONFLICT OF INTEREST

There is no conflict of interest in this study.

REFERENCES

- [1] Cinar C, Oran I. "Intrakraniyal Dissekan ve Travmatik Anevrizmalarda Tedavi", *Türk Radyoloji Semin*,10,115–27,(2022).
- [2] Li MH, Chen SW, Li YD, Chen YC, Cheng YS, Hu DJ, et al. "Prevalence of unruptured cerebral aneurysms in Chinese adults aged 35 to 75 years: A cross-sectional study", *Ann Intern Med* (2013).
- [3] Wei X, Jiang J, Cao W, Yu H, Deng H, Chen J, et al. Artificial intelligence assistance improves the accuracy and efficiency of intracranial aneurysm detection with CT angiography. *Eur J Radiol*, 149,110169,(2022).
- [4] Greving JP, Wermer MJH, Brown RD, Morita A, Juvela S, Yonekura M, et al. "Development of the PHASES score for prediction of risk of rupture of intracranial aneurysms: a pooled analysis of six prospective cohort studies" *Lancet Neurol*, 13,59–66,(2014).
- [5] Mensah E, Pringle C, Roberts G, Gurusinge N, Golash A, Alalade AF" Deep Learning in the Management of Intracranial Aneurysms and Cerebrovascular Diseases: A Review of the Current Literature", *World Neurosurg*, (2022).
- [6] Gu F, Wu X, Wu W, Wang Z, Yang X, Chen Z, et al. "Performance of deep learning in the detection of intracranial aneurysm: A systematic review and meta-analysis", *Eur J Radiol* , 155:110457,(2022).
- [7] Wang J, Ti L, Sun X, Yang R, Zhang N, Sun K. DSA "Image Analysis of Clinical Features and Nursing Care of Cerebral Aneurysm Patients Based on the Deep Learning Algorithm". *Scanning*, 1–6,(2022).
- [8] Brisman JL, Song JK, Newell DW. "Cerebral Aneurysms" *N Engl J Med*. 355:928–39,(2006).
- [9] Heit JJ, Honce JM, Yedavalli VS, Bacim CE, Tatit RT, Copeland K, et al. "RAPID Aneurysm: Artificial intelligence for unruptured cerebral aneurysm detection on CT angiography", *J Stroke Cerebrovasc Dis*,31:106690,(2022).
- [10] Silva MA, Patel J, Kavouridis V, Gallerani T, Beers A, Chang K, et al. "Machine Learning Models can Detect Aneurysm Rupture and Identify Clinical Features Associated with Rupture", *World Neurosurg*,131,e46–51,(2019).
- [11] Buchlak OD, Milne MR, Seah J, Johnson A, Samarasinghe G, Hachey B, et al. "Charting the potential of brain computed tomography deep learning systems", *J Clin Neurosci*, (2022).
- [12] Duan H, Huang Y, Liu L, Dai H, Chen L, Zhou L. "Automatic detection on intracranial aneurysm from digital subtraction angiography with cascade convolutional neural networks", *Biomed Eng Online*, 18:110,(2019).
- [13] Liao J, Liu L, Duan H, Huang Y, Zhou L, Chen L, et al. "Using a Convolutional Neural Network and Convolutional Long Short-term Memory to Automatically Detect Aneurysms on 2D Digital Subtraction Angiography Images: Framework Development and Validation", *JMIR Med Informatics*, (2022).
- [14] Hu T, Yu J, Yang H, Ni W. "Segmentation of Intracranial Aneurysm Based on U-Net and BiConvGRU. Proc" - *14th Int. Congr. Image Signal Process. Biomed. Eng. Informatics*, CISP-BMEI ,(2021).
- [15] Mei Y jia, Hu R ting, Lin J, Xu H yu, Wu L ya, Li H peng, et al. "Diagnosis of Middle Cerebral Artery Stenosis Using Transcranial Doppler Images Based on Convolutional Neural Network", *World Neurosurg* (2022).
- [16] Dai X, Huang L, Qian Y, Xia S, Chong W, Liu J, et al. "Deep learning for automated cerebral aneurysm detection on computed tomography images", *Int J Comput Assist Radiol Surg* (2020).
- [17] Di Noto T, Marie G, Tourbier S, Alemán-Gómez Y, Esteban O, Saliou G, et al. "Towards Automated Brain Aneurysm Detection in TOF-MRA: Open Data, Weak Labels, and Anatomical Knowledge". *Neuroinformatics*, (2022).

- [18] Ou C, Qian Y, Chong W, Hou X, Zhang M, Zhang X, et al. "A deep learning-based automatic system for intracranial aneurysms diagnosis on three-dimensional digital subtraction angiographic images", *Med Phys* (2022).
- [19] Ivantsits M, Goubergrits L, Kuhnigk JM, Huellebrand M, Bruening J, Kossen T, et al. "Detection and analysis of cerebral aneurysms based on X-ray rotational angiography - the CADA 2020 challenge". *Med Image Anal.* (2022).
- [20] Sathish Kumar L, Hariharasitaraman S, Narayanasamy K, Thinakaran K, Mahalakshmi J, Pandimurugan V. "AlexNet approach for early stage Alzheimer's disease detection from MRI brain images", *Mater. Today Proc.*, (2021).
- [21] Darici MB. "Performance Analysis of Combination of CNN-based Models with Adaboost Algorithm to Diagnose Covid-19 Disease", *Politeknik Dergisi* 26,179-90,(2023).
- [22] Biçer MB, Eliyi U, Türsel Eliyi D. "Deep Learning-based Classification of Breast Tumors using Raw Microwave Imaging Data", *Journal of Polytechnic* (2023).
- [23] Tümay M, Civelek Z, Teke M. Glakom ve Katarakt "Hastalığının Derin Öğrenme Modelleri ile Teşhisi", *Journal of Polytechnic*, (2023).
- [24] Akbulut H, Aslantaş V. "Evrişimli sinir ağı kullanarak çoklu-pozlamalı görüntü birleştirme", *Gazi Üniversitesi Mühendislik Mimar Fakültesi Dergisi* 38,1439-52,(2023).
- [25] Gupta K, Bajaj V. "Deep Learning Models-Based CT Scan Image Classification for Automated Screening of COVID-19", *SSRN Electron J*, (2022).

ERKEN GÖRÜNÜM